

DISTRIBUTED COMPUTATION OF PERSISTENT COHOMOLOGY

PREPRINT, COMPILED OCTOBER 23, 2024

Arnur Nigmatov, Dmitriy Morozov
Lawrence Berkeley National Laboratory
anigmatov@lbl.gov, dmorozov@lbl.gov

ABSTRACT

Persistent (co)homology is a central construction in topological data analysis, where it is used to quantify prominence of features in data to produce stable descriptors suitable for downstream analysis. Persistence is challenging to compute in parallel because it relies on global connectivity of the data. We propose a new algorithm to compute persistent cohomology in the distributed setting. It combines domain and range partitioning. The former is used to reduce and sparsify the coboundary matrix locally. After this initial local reduction, we redistribute the matrix across processors for the global reduction. We experimentally compare our cohomology algorithm with DIPHA, the only publicly available code for distributed computation of persistent (co)homology; our algorithm demonstrates a significant improvement in strong scaling.

1 INTRODUCTION

Topological data analysis is a research area at the intersection of computational geometry and algebraic topology. It aims to understand the “shape of data” by identifying prominent topological features that are stable to perturbations. One of its central constructions is persistent (co)homology [11, 12], which achieves this aim by examining the data across a range of scales and keeping track of the values where features are born and die. By pairing these events, it generates a *persistence diagram*, which is a stable descriptor that summarizes the distribution of topological features as a point set in the plane.

Persistence has found numerous applications. In cosmology, it’s been used to describe the shape of the Cosmic Web [23]—the distribution of matter forming the large-scale structure of the Universe—and thus to compare different cosmological models. In materials science, persistence has been used to detect cavities and channels in nanoporous materials, information that was in turn used as an input for a machine learning algorithm to predict adsorption of a greenhouse gas [16]. In machine learning, persistence has been used to regularize the training loss [6, 21] to reduce topological complexity of the decision boundary, and thus minimize the model overfitting to outliers.

Some of the applications of persistence require processing very large data sets. For example, cosmological simulations are some of the largest users of modern supercomputers, modeling domains on the order of $8,192^3$ grid cells. In other applications, even when the input data set is small, the combinatorial construction of simplicial complexes required to represent it for the persistence computation explodes the input complexity, scaling exponentially with homological dimension. These observations highlight the need for distributed algorithms and software to compute persistence, both to improve the running times and to gain access to the distributed (multi-node) memory.

Two types of distributed algorithms have been proposed in the literature. The first [17] partitions data by domain, processes as much of the computation locally as possible, and then performs a reduction among all processes to deduce the global

connectivity of the topological features. The global reduction uses a gluing procedure called *Mayer–Vietoris blowup complex*, which adds extra cells to represent the structure of the intersecting regions of the domain. Algebraically, it can be interpreted as iterating through the Mayer–Vietoris spectral sequence [4]. The approach suffers from Amdahl’s law: for small number of processors, the computation scales very well, since the local work dominates, but the running time quickly plateaus as the global gluing dominates the work and additional processes cannot help [17].

The second approach partitions the data by function value. The algorithm is based on the spectral sequence of the filtration [11]; it is implemented in the only publicly available code for this problem, DIPHA [2, 24]. The input matrix is reduced by blocks, moving away from the diagonal. This guarantees that each process only needs to access the data in the range it is responsible for and can pass the data to its neighbors, when the reduction leaves its local range.

Other techniques are available in shared memory, for example, identification of apparent pairs [18, 27] or waitfree column reduction that uses atomic operations for synchronization [19], but these do not help in the distributed memory setting.

Our contribution is three-fold.

1. We show that if one switches from persistent homology to persistent cohomology, the coboundary matrix that serves as input to the computation has exactly the same structure as the boundary matrix of the blowup complex. Thus, the algorithm of [17] can be applied to it directly, and we use its first round to locally reduce data partitioned by the domain.
2. We combine the two approaches and after one round of local domain reduction, we switch to the spectral sequence algorithm to reduce the data globally.
3. We demonstrate that the combined approach scales significantly better than the persistent cohomology implementation in DIPHA.

2 BACKGROUND

2.1 Simplicial Complexes

We start with a finite *vertex set* V . For instance, V can be the set of nodes of a grid, on which a numerical simulation evaluates some function f . A k -*simplex* is a set of $k + 1$ vertices. If $(k - 1)$ -simplex τ is a subset of k -simplex σ , $\tau \subset \sigma$, then τ is called a *facet* of σ . The set of all facets of σ forms its *boundary*, denoted $\partial\sigma$. For simplicity, we work with mod 2 coefficient (in $\mathbb{Z}/2\mathbb{Z}$), and we treat the boundary as a formal sum:

$$\partial\sigma = \sum_{\tau \subset \sigma, |\sigma \setminus \tau|=1} \tau.$$

The set of simplices K is called a *simplicial complex*, if for each $\sigma \in K$ it also contains all facets of σ (and hence, recursively, all subsets of σ). A *filtration* of K is a function on the simplicial complex, $f: K \rightarrow \mathbb{R}$, such that $f(\tau) \leq f(\sigma)$ whenever $\tau \subset \sigma$. We call $f(\sigma)$ the *filtration value* of σ .

A specific construction, common for scientific computing data, that we use in our experiments is called a *lower-star* filtration. It extends a function $\hat{f}: V \rightarrow \mathbb{R}$ defined on the vertices (e.g., of a simulation domain) to a filtration $f: K \rightarrow \mathbb{R}$, defined on all the simplices (in the triangulation of the domain). It assigns to each simplex the maximum value of its vertices,

$$f(\sigma) = \max(\hat{f}(v_0), \hat{f}(v_1), \dots, \hat{f}(v_k)).$$

Here $\sigma = \{v_0, \dots, v_k\}$. Lower-star filtrations are used to capture the topology of sublevel sets, $f^{-1}(-\infty, a]$ of scalar function.

Lower-star filtrations highlight that f need not be injective. However, the computation of persistence requires a total order. So we assume that all values of f are distinct, and every simplex is uniquely determined by its value $f(\sigma)$. To achieve this in practice, we assign a unique identifier `uid` to each simplex and break ties by comparing the pairs $(f(\sigma), \text{uid}(\sigma))$ lexicographically.

2.2 Coboundary matrix

For a fixed simplicial complex K , simplex τ is in the coboundary of σ if and only if σ is in the boundary of τ . The set of all simplices $\tau \in K$ such that $\sigma \in \partial\tau$ is called the *coboundary* of σ . Suppose that we have a total order on the simplices of K (given by some filtration). We enumerate the simplices of K in *reverse* filtration order and define the *coboundary matrix* of K by the formula $D[i, j] = 1$ if and only if the j -th simplex is in the coboundary of the i -th simplex (in other words, the *rows* of D encode the boundaries). It is often convenient to extend the notation and use simplices themselves to refer to the matrix entries: $D[\sigma, \tau]$ means $D[i, j]$ when σ has index i and τ has index j in the reverse filtration order.

Remark. We work with the most common case of $\mathbb{Z}/2\mathbb{Z}$ coefficients, which allows us to treat rows and column of all our matrices as sets of simplices. The theory of persistent homology is valid for arbitrary fields, and all algorithms in the paper can be trivially re-written for any $\mathbb{Z}/p\mathbb{Z}$ (p prime).

2.3 Sequential algorithm

We write $A[k]$ to denote the k -th column of matrix A and $A[k, \cdot]$ to denote the k -th row of A . The index of the last non-zero entry of a column is denoted $\text{low}(A[k])$; for zero columns, low is undefined. We say that two columns have a *collision*, if they have the same low . Matrix A is called *reduced*, if there are no collisions. A *valid* column operation is adding a column from left to right: $A[k] \leftarrow A[k] + A[k']$ when $k' < k$. We usually perform this operation, if columns k and k' have a collision. In this case, this operation eliminates the collision, and either $A[k] = 0$ or $\text{low}(A[k]) < \text{low}(A[k'])$. A *reduction* is any sequence of valid operations that brings matrix A to a reduced form.

Algorithm 1 presents a pseudocode for a generic reduction. As written, it is not sufficiently detailed to be an algorithm: we do not specify the order in which **for all** iterates over the columns $R[i]$. Nor do we specify a concrete choice of a column to the left $R[j]$ that has a collision with $R[i]$ (there can be more than one).

The usual way to check existence of column $R[j]$ that has a collision with $R[i]$ (current column being reduced) is to maintain a table of *pivots*: given a row index a , the entry `pivots[a]` contains the index of a column with $\text{low}(R[\text{pivots}[a]]) = a$. If no such column has been seen by the algorithm, `pivots[a] = -1`. If we process all columns from left to right and, once a column cannot be further reduced, mark it as a pivot, we obtain the standard reduction algorithm [10]. Its pseudocode is in Algorithm 2.

From a reduced matrix, one obtains a *persistence pairing*: simplices σ and τ form a pair, if $\text{low}(R[\sigma]) = \tau$. Simplex σ is called *negative* and simplex τ is *positive*. Every simplex can appear in at most one pair; in particular, if τ is positive, then its column $R[\tau]$ must be 0.¹ The *persistence diagram* of K in dimension d is defined as the multi-set of all pairs $(f(\sigma), f(\tau)) \in \mathbb{R}^2$ such that simplices σ and τ are paired, σ is a d -simplex (hence τ must be a $d + 1$ -simplex) and $f(\sigma) \neq f(\tau)$. Although a reduced matrix is not unique, the pivots are, and so all reduced matrices produce the same persistence pairing [7].

Algorithm 1 Reduction algorithm.

```

1: function REDUCEMATRIX( $D$ )
2:    $R \leftarrow D$ 
3:   for all column  $R[i]$  of  $R$  do
4:     while  $R[i] \neq 0$  do
5:       while  $\exists j < i : \text{low}(R[j]) = \text{low}(R[i])$  do
6:          $R[i] \leftarrow R[i] + R[j]$ 
7:   return  $R$ 
8: end function

```

2.4 Clearing

Clearing was first suggested in [5]. The idea follows from the structure of the (co)boundary matrix: if we know that a simplex σ is positive, then we do not need to reduce its column—it has to be 0. When computing cohomology, after reducing the coboundary matrix of k -simplices, we can identify all the $(k +$

¹This follows from the fundamental property of the (co)boundary operator: its composition with itself is 0.

Algorithm 2 Reduction algorithm.

```

1: function REDUCEMATRIXELZ( $D$ )
2:    $R \leftarrow D$ 
3:    $m, n \leftarrow$  number of rows and columns of  $R$ 
4:    $\text{pivots} = [-1, -1, \dots, -1]$  // array of length  $m$ 
5:   for  $c \in [1, 2, \dots, n]$  do
6:     while  $R[c] \neq 0$  do
7:        $\ell \leftarrow \text{low}(R[c])$ 
8:        $p \leftarrow \text{pivots}[\ell]$ 
9:       if  $p \neq -1$  then
10:         $R[c] = R[c] + R[p]$ 
11:      else
12:         $\text{pivots}[\ell] \leftarrow c$ 
13:      break
14:   return  $R$ 
15: end function

```

1)-simplices that appear as pivots low of some column and then set their columns to 0 before reducing them in dimension $k + 1$.

3 ALGORITHM

As is often the case in applications, we assume our input data is spatially partitioned. We model this as a cover of the domain with sub-complexes. To make this precise, we use the following notation. Let K be a simplicial complex covered by simplicial sub-complexes K_i , $K = \bigcup_i K_i$. A simplex σ is called *interior* to K_i , if it belongs only to K_i and no other sub-complex, $\sigma \in K_i \setminus (\bigcup_{j \neq i} K_j \cap K_i)$. The rest of the simplices, $\bigcup_{j \neq i} (K_j \cap K_i)$, are called *shared*. The intersection of simplicial complexes is a simplicial complex; therefore, a simplex is shared if and only if all of its vertices are shared. If at least one vertex of a simplex lies in the interior $K_i \setminus (\bigcup_{j \neq i} K_j \cap K_i)$, then the simplex is interior.

The coboundary matrix D_i of K_i consists of two parts.² The columns of the interior simplices in D_i consist entirely of interior simplices and, therefore, they are the same as in the full coboundary matrix of K . The columns of shared simplices in D_i are subsets of the full columns in D ; the rows of simplices outside K_i are missing.

After the initial local reduction of matrices D_i , we assemble the full matrix D , partitioned among the processors. Let N be the number of columns of D , p be the number of processors. We make processor i responsible for the column and row range $[s_i, s_{i+1})$, where the sequence

$$-\infty = s_{-1} < s_0 < s_1 < \dots < s_{p-1} < s_p = \infty$$

is computed to split the number of columns between processors approximately evenly. We use a sample sort to identify the splitters. Finding a rank that is responsible for value v is done by binary search, as expressed in Algorithm 3.

The overall algorithm, expressed in pseudocode in Algorithm 4, consists of three parts:

²Normally it would be denoted D_i^\perp to distinguish it from the boundary matrix, but we only work with cohomology in this paper, so we drop the \perp superscript everywhere for convenience.

Algorithm 3 Obtain rank by value.

```

1: function RANKBYVALUE( $v$ )
2:    $r \leftarrow$  first  $i$  such that  $s_{i-1} \leq v < s_i$ 
3:   //  $r$  is found by binary search
4:   return  $r$ 
5: end function

```

Algorithm 4 Full Algorithm

```

1:  $R_i \leftarrow \text{REDUCELOCAL}(K_i)$ 
2:  $[s_{-1}, \dots, s_p] \leftarrow \text{SAMPLESORT}(\text{all simplex values})$ 
3:  $R^F \leftarrow \text{REDISTRIBUTE COLUMNS}(R_i, [s_{-1}, \dots, s_p])$ 
4:  $R^F \leftarrow \text{REDUCE}(R^F)$ 
5:  $\text{all\_done} \leftarrow \text{False}$ 
6:  $\text{round} \leftarrow 1$ 
7:  $\text{updated} \leftarrow \emptyset$ 
8: for  $\text{dim} = 0.. \text{max\_dim}$  do
9:   while not  $\text{all\_done}$  do
10:     $\text{SEND COLUMNS}(\text{dim}, \text{updated}, \text{round})$ 
11:     $\text{all\_done} \leftarrow$  none of the ranks sent a column
12:     $\text{updated} \leftarrow \text{RECEIVE COLUMNS}$ 
13:     $\text{round} \leftarrow \text{round} + 1$ 
14:   $\text{CLEAR COLUMNS}(\text{dim})$ 

```

1. Local reduction and sparsification. We reduce each D_i on a separate processor and then sparsify it, as discussed in Sections 3.1 and 3.2. At this phase, rank i has the columns of D that correspond to simplices in cover sub-complex K_i (domain partitioning). The columns of shared simplices are incomplete.
2. Rearranging matrix across ranks in filtration order. After determining the splitters s_i via a sample sort, the processors exchange their domain partitioned columns, to partition them by function value. Rank i gathers a contiguous chunk of columns of D whose **column values** are in $[s_{i-1}, s_i)$. All columns are now complete (they include both interior and shared simplices). Each rank runs a local reduction on its own chunk once.
3. Global reduction. At this step, rank i becomes responsible for the columns whose low belongs to segment $[s_{i-1}, s_i)$. In a reduction loop, each rank (a) receives columns sent to it, (b) runs a local reduction using these received columns, (c) sends columns whose low is not in $[s_{i-1}, s_i)$ to the rank responsible for it. The loop finishes when all columns are reduced.

3.1 Local Reduction: Matrix Structure

The initial local computations of our algorithm are as in [17]. We denote by \hat{D}_i the submatrix of D_i formed by the columns that correspond to the interior simplices. We denote by D_i^S the submatrix of D_i formed by the columns that correspond to shared simplices. The coboundary of a shared simplex can contain both shared and interior simplices. We split D_i^S further into the submatrix \hat{D}_i^S formed by the rows of interior simplices and D_i^{SS} formed by the rows of shared simplices. See Figure 1. The order of columns and rows inside each \hat{D}_i , \hat{D}_i^S and D_i^{SS} is the same as in D_i .

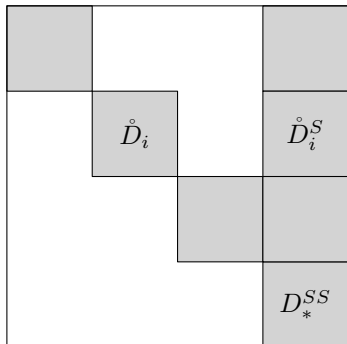


Figure 1: The overall structure of the coboundary matrix D . Non-zero blocks are highlighted in gray, and different blocks of submatrix D_i are labeled. D_*^{SS} contains rows and columns from D_i^{SS} for all i . This coboundary matrix structure is the same as the boundary matrix structure of the blowup complex used in [17].

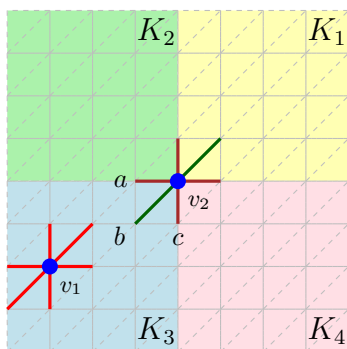


Figure 2: A triangulation of a 2-dimensional grid, partitioned among four processes. The four cover sub-complexes are shown in four colors. Coboundaries of interior (v_1) and shared (v_2) simplices are illustrated.

An example is given in Figure 2. The global domain is split between 4 ranks. We use Freudenthal triangulation to create a simplicial complex K on the regular grid (dashed lines), covered by the four sub-complexes K_1, \dots, K_4 . The coboundary of an interior vertex v_1 consists of the 6 highlighted edges, all interior. The part of the coboundary of a shared vertex v_2 that belongs to sub-complex K_3 , and therefore to the coboundary matrix D_3 on rank 3, consists of two shared edges $\{a, v_2\}$ and $\{c, v_2\}$ and one interior edge $\{b, v_2\}$. This example also illustrates why none of the ranks have complete columns of D for the shared simplices.

Crucially, only the rows of simplices interior to K_i have non-zero entries in \hat{D}_i . In other words, each rank has complete columns of the global coboundary matrix D that correspond to its interior simplices. Therefore, rank i can locally reduce matrix \hat{D}_i . However, there is no way to guarantee (yet) that a local pair (σ, τ) identified from the reduced \hat{D}_i is a true global pair.

Algorithm 5 contains pseudocode for the local part. Since we do not run any reduction operations on the columns of D_i^S , and all further parts of the algorithm operate on matrix R which was initially D , in the pseudocode we directly write the columns of matrices \hat{D}_i^S and D_i^{SS} into the corresponding matrices \hat{R}_i^S, R_i^{SS} .

Algorithm 5 Local Reduction.

```

1: function REDUCELOCAL( $K_i$ )
2:    $D_i \leftarrow$  coboundary matrix of  $K_i$ 
3:    $\hat{D}_i \leftarrow$  empty matrix
4:    $D_i^S \leftarrow$  empty matrix
5:   for all columns  $D_i[\sigma]$  of  $D_i$  do
6:     if  $\sigma$  is interior then
7:       append  $D_i[\sigma]$  to  $\hat{D}_i$ 
8:     else
9:       append empty columns to  $\hat{R}_i^S, R_i^{SS}$ 
10:    for all entries  $\tau$  of  $D_i[\sigma]$  do
11:      if  $\tau$  is interior then
12:        append  $\tau$  to the last column of  $\hat{R}_i^S$ 
13:      else
14:        append  $\tau$  to the last column of  $R_i^{SS}$ 
15:    $\hat{R}_i \leftarrow$  REDUCEMATRIXELZ( $\hat{D}_i$ )
16: end function

```

3.2 Local Reduction: Ultrasparsification

Ultrasparsification is a procedure described in [17] that allowed its authors to lower both the space and time complexity of the global hierarchical reduction for spatially partitioned data. The idea is to zero out all but one elements of the interior columns via row operations. The validity of this operation, stated in the following lemma, follows from [7].

Lemma 1. *The persistence pairing determined by R does not change, if in the reduction process we also perform row operations $R[i, \cdot] \leftarrow R[i, \cdot] + R[j, \cdot]$ provided that we add rows bottom-up, $j > i$.*

When we are done reducing a column $R[k]$, we can add the row $\text{low}(R[k])$ to all other rows j such that $R[j, k] \neq 0$. As a result, the only non-zero entry remaining in the column is the pivot. In a sequential algorithm, this would add extra work, but it would produce the same persistence pairing. In the distributed setting, this procedure both reduces the size of the columns that we send between ranks and makes column addition faster.

In our setting, we can perform this operation locally, because each rank i has complete rows of matrix D that correspond to the simplices of K_i . Since we split the local matrix into parts, we must apply row additions simultaneously to \hat{R}_i and \hat{R}_i^S . Note that R_i^{SS} , which is shared among multiple ranks, remains untouched. A convenient optimization is to perform ultrasparsification itself bottom-up, starting with the column of \hat{R}_i whose low is maximal. Then we do not actually need to do any computations on \hat{R}_i , because we maintain the invariant: when we add row ℓ to row t above it, the only non-zero element in row ℓ is the lowest one of the column that we are processing, so we can just remove all elements from the column of \hat{R}_i except for the lowest one. We must, however, perform a row addition on \hat{R}_i^S . So, while the interior columns become ultrasparse, the columns of shared simplices can actually become denser.

We perform one more operation to sparsify the columns of \hat{R}_i^S . In the global matrix R , the columns of \hat{R}_i and \hat{R}_i^S are interleaved, following the reverse filtration order. Since we can always per-

form column operations, we can add the ultrasparse column $\mathring{R}_i[t]$ to every column of \mathring{R}_i^S that succeeds it in the reverse filtration order and contains $x = \text{low}(\mathring{R}_i[t])$. This operation removes x from the column \mathring{R}_i^S .

Figure 3 illustrates the overall procedure. We write $\alpha < \beta$ to indicate that in the global matrix R the column of α precedes the column of β . Global order of simplices in matrix R corresponds to simplex indices: $\sigma_i < \sigma_{i+1}$ for $i = 1, \dots, 4$. We start the ultrasparsification at column $\mathring{R}_i[\sigma_4]$ because its pivot is the lowest. We add the row of τ_3 to the rows of τ_2 and τ_1 to remove all non-zero entries from the column. We must perform the same additions on the rows of \mathring{R}_i^S . Then we sparsify the column $\mathring{R}_i[\sigma_2]$. After the columns of \mathring{R}_i are ultrasparse, we can perform column operations to sparsify the rows. We add column $\mathring{R}_i[\sigma_2]$ to all columns of \mathring{R}_i^S that are to the right from it and contain 1 in row τ_2 (in the figure, we remove τ_2 from both columns $\mathring{R}_i^S[\sigma_3]$ and $\mathring{R}_i^S[\sigma_5]$). When we sparsify the row of τ_3 , we cannot add $\mathring{R}_i[\sigma_4]$ to $\mathring{R}_i^S[\sigma_1]$, because σ_4 is to the left from σ_1 , so we can only remove one entry by adding $\mathring{R}_i[\sigma_4]$ to $\mathring{R}_i^S[\sigma_5]$.

Pseudocode for this procedure is given in Algorithm 6. Here we slightly abuse the notation: since we work over $\mathbb{Z}/2\mathbb{Z}$, we treat columns as sets.

Algorithm 6 Ultrasparsification.

```

1: function SPARSIFY( $\mathring{R}_i, \mathring{R}_i^S$ )
2:    $L \leftarrow$  sorted  $\{\text{low}(\mathring{R}_i[c]) \mid \text{non-zero columns } c \text{ of } \mathring{R}_i\}$ 
3:   for  $\ell \in L$  do
4:     //  $t$  the column of  $\mathring{R}_i$  whose low is  $\ell$ 
5:      $t \leftarrow$  pivots[ $\ell$ ]
6:     for all  $e \in R[t]$  except  $\ell$  do
7:        $\mathring{R}_i^S[e, \cdot] \leftarrow \mathring{R}_i^S[e, \cdot] + \mathring{R}_i^S[\ell, \cdot]$ 
8:       // the only entry left is low
9:        $\mathring{R}_i[t] \leftarrow \{\ell\}$ 
10:    for all column  $\mathring{R}_i^S[j]$  of  $\mathring{R}_i^S$  do
11:      for all entry  $e \in \mathring{R}_i^S[j]$  do
12:        if  $\exists p$  s.t.  $\text{low}(\mathring{R}_i[t]) = e$  and  $p < j$  then
13:          // removes  $e$  from  $\mathring{R}_i^S[j]$ 
14:           $\mathring{R}_i^S[j] \leftarrow \mathring{R}_i^S[j] + \mathring{R}_i^S[p]$ 
15: end function

```

3.3 Rearranging

When we compute local coboundary matrix D_i , we only have access to the values of simplices in K_i . Suppose

$$K_i = \{\sigma_1^i, \dots, \sigma_{N_i}^i\},$$

where we list simplices in the reverse filtration order:

$$v_1^{(i)} > \dots > v_{N_i}^{(i)}, \text{ where } v_t^{(i)} = f(\sigma_t^i).$$

In the compressed column representation, if a column of D_i is $[a_1, a_2, \dots]$, $0 \leq a_1 < a_2 < \dots$, it means that it contains simplices $\sigma_{a_1}^i, \sigma_{a_2}^i$, etc. In order to perform the global reduction, we must use consistent global indexing of simplices. If we order

all simplices following the filtration,

$$K = \{\sigma_1, \dots, \sigma_N\}, \text{ and } v_1 > \dots > v_N, \text{ where } v_t = f(\sigma_t),$$

then, since $K = \bigcup K_i$, every simplex σ_t^i in the local order of K_i maps to some $\sigma_{t'}$ in the global order,

$$\forall i \in \{1, \dots, p\}, \forall t \in \{1, 2, \dots, N_i\}, \exists! t' \text{ such that } \sigma_t^{(i)} = \sigma_{t'}.$$

This generates a monotonically increasing map,

$$r_i: \{1, \dots, N_i\} \rightarrow \{1, \dots, N\}, \quad t \mapsto t'.$$

To go from matrices R_i to a global matrix R , we must translate all entries using the map r_i .

This approach is not feasible in practice: it requires having the sorted values, $\{v_1, \dots, v_N\}$, of the entire domain in the memory of each rank. This is impossible for large datasets, especially when we take into account that the reduction algorithm is itself memory-intensive.

An alternative strategy is to avoid integral indices and to store the values themselves: instead of having columns of R^F of the form $[a_1, a_2, \dots]$, where a_t is the global index of $\sigma_t \in K$, we will represent the columns as sorted arrays of values v_t directly. The complexity of column addition does not change; it is the same symmetric difference.

Algorithm 7 Rearranging Matrix.

```

1: function REDISTRIBUTE_COLUMNS( $R_i$ )
2:   for all columns  $R_i[\sigma]$  of  $R_i$  do
3:      $r \leftarrow$  RANKBYVALUE( $\text{low}(R_i[\sigma])$ )
4:     convert  $R_i[\sigma]$  from indices to values
5:     send  $R_i[\sigma]$  to  $r$ 
6:   for all incoming columns  $R_k[\sigma]$  do
7:     // merge  $R_k[\sigma]$  into  $R^F$ 
8:     if  $R^F$  already has column for  $\sigma$  then
9:        $R^F[\sigma] \leftarrow R_k[\sigma] \cup R^F[\sigma]$ 
10:    else
11:       $R^F[\sigma] \leftarrow R_k[\sigma]$ 
12:     $R^F \leftarrow$  REDUCEMATRIXELZ( $R^F$ )
13: end function

```

Many columns are zeroed by local reduction, so we choose to represent the global matrix not as an `std::vector` of `std::vectors`, but as an `std::map` that uses column values as keys. The columns themselves are still stored as `std::vectors` of values. The fact that a `map` is ordered makes iterating over columns in the filtration order easy. If during the global reduction a column becomes zero, we remove it from the `map` entirely, to avoid storing empty vectors.

We must eliminate all collisions between columns in the whole matrix. Therefore, it is convenient to rearrange columns among ranks according to the values `low` of their pivots (this idea was proposed in [2]). We cannot determine this assignment immediately after the local reduction step: ranks do not have complete columns for shared simplices. Before we go into the global reduction loop, we rearrange the matrix according to column values: the column of σ is sent to rank i such that $f(\sigma) \in [s_{i-1}, s_i]$. When a rank receives columns, it needs to merge different parts of a column together. The ultrasparsification procedure does not create any conflicts, because each rank was operating on

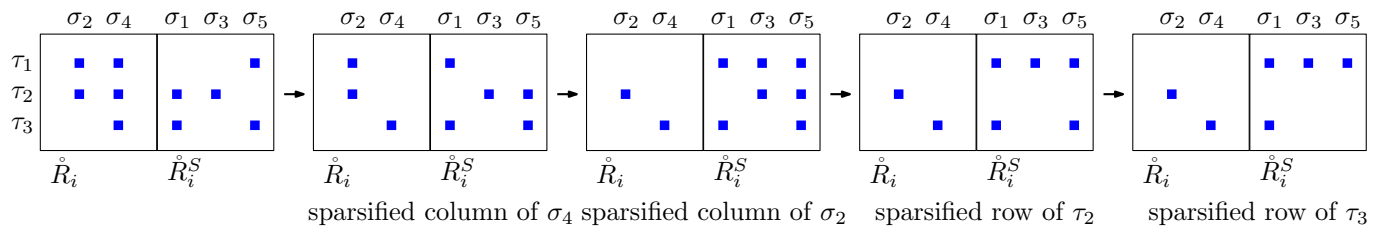


Figure 3: Illustration of the ultrasparsification procedure.

the rows that correspond to its interior simplices. After we assemble a contiguous chunk of columns R^F on each rank, we run a local reduction on this chunk again. The pseudocode for this part is in Algorithm 7. To avoid additional verbosity, in this algorithm we do not explicitly state that columns of the local matrix R_i are actually split between \hat{R}_i , \hat{R}_i^S and R_i^{SS} .

3.4 Global reduction loop

The main reduction loop is conceptually simple: rank i receives columns whose low belongs to the range $[s_{i-1}, s_i)$ and reduces them until there are no more collisions among local columns. Columns that were reduced to zero are removed from the map; non-zero columns are sent to the rank responsible for their new low. Note that when we reduce a column, its low only gets smaller (moves up in the matrix). Therefore we only send columns from rank i to rank $j < i$.

There is one exception: in the first iteration of the loop, we must send all columns to new ranks. Recall that after rearranging column $R[\sigma]$ is on the rank that corresponds to $f(\sigma)$, not to the value of its low. In all other iterations, we must send every column whose low moved out of $[s_{i-1}, s_i)$ after we received columns and reduced them. These columns are contained in the updated argument in Algorithm 8.

The local reduction procedure is slightly more complicated than the standard reduction. In Algorithm 2, when we reduce column $R[\sigma]$ and query the pivots table for $\text{pivots}[\text{Low}(R[\sigma])]$, the column in the table is always to the left. In the global reduction loop, we may receive columns that lie to the left of us in the global order, and so the existing pivot may lie to the right; see Figure 4 for an illustration. In this case, we mark the column we are reducing as the new pivot and switch to reducing the column to the right that was marked as the pivot before. This algorithm is closely related to the algorithm in [19], where it is used for shared-memory parallelism. Its adaptation to our setting makes it simpler and obviates the need for atomic operations and complicated memory management. The resulting pseudocode is in Algorithm 9.

4 CLEARING

An important aforementioned optimization is clearing: zeroing out columns of positive simplices without reducing them explicitly. Applying it during the initial local phase is straightforward. If the row of some simplex σ contains the lowest non-zero entry of at least one column, this will be true until the end of the reduction (either there will be no collisions, or this particular lowest one will be killed by adding another column *with*

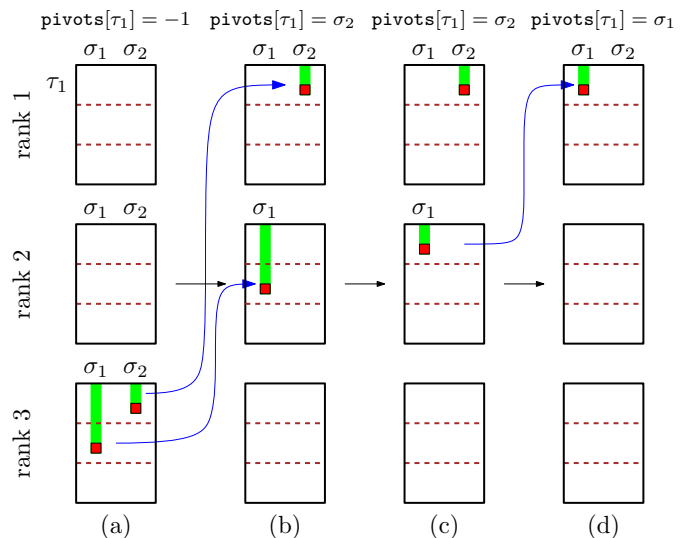


Figure 4: An example of the pivot to the right situation. (a) Rank 3 has $R[\sigma_1]$ and $R[\sigma_2]$. Rank 1 does not have any column whose low is τ_1 , so in its local pivots table the corresponding entry is -1 . (b) Based on their low values, rank 3 sends the columns to ranks 2 and 1, respectively. (c) After the local reduction, on rank 1, $R[\sigma_2]$ has no collisions, so σ_2 remains a pivot for τ_1 . Rank 2 reduces $R[\sigma_1]$ (via columns that are not shown) and its new low is now τ_1 . (d) Rank 2 sends $R[\sigma_1]$ to rank 1. Now, when rank 1 runs local reduction on $R[\sigma_1]$, its local pivots table points to $R[\sigma_2]$ which is *to the right* from σ_1 .

Algorithm 8 Sending columns in global reduction.

```

1: function SENDCOLUMNS(dim, updated, round)
2:   if round = 1 then
3:     // first round: rearrange all columns by low
4:     for all column  $R^F[\sigma]$  of  $R^F$  in dimension dim do
5:        $r \leftarrow \text{RANKBYVALUE}(\text{Low}(R^F[\sigma]))$ 
6:       send  $R^F[\sigma]$  to rank  $r$ 
7:   else
8:     for all column  $R^F[\sigma]$  where  $\sigma \in \text{updated}$  do
9:       // guaranteed:  $\dim(\sigma) = \dim$ 
10:       $r \leftarrow \text{RANKBYVALUE}(\text{Low}(R^F[\sigma]))$ 
11:      send  $R^F[\sigma]$  to rank  $r$ 
12: end function

```

Algorithm 9 Receiving Columns in Distributed Reduction.

```

1: function RECEIVECOLUMNS( $C$ ) //  $C$ : received columns
2:   updated  $\leftarrow \emptyset$ 
3:    $\sigma \leftarrow$  leftmost of all columns in  $C$  // we start reduction
   from  $\sigma$ 
4:   insert columns of  $C$  into  $R^F$ 
5:   while true do
6:     if  $\sigma$  is not the last column in  $R^F$  then
7:        $\sigma_{next} \leftarrow$  next simplex after  $\sigma$  in  $R^F$ 
8:     else
9:        $\sigma_{next} \leftarrow \sigma$ 
10:    while  $R^F[\sigma] \neq 0$  do
11:       $\ell \leftarrow \text{low}(R^F[\sigma])$ 
12:      if pivots[ $\ell$ ] <  $\sigma$  and pivots[ $\ell$ ]  $\neq -1$  then
13:        // Pivot to the left, standard reduction
14:         $R^F[\sigma] \leftarrow R^F[\sigma] + R^F[\text{pivots}[\ell]]$ 
15:      else if pivots[ $\ell$ ] >  $\sigma$  then
16:        // Pivot to the right, switch to reducing col-
umn pivots[ $\ell$ ]
17:        SWAP(pivots[ $\ell$ ],  $\sigma$ )
18:         $R^F[\sigma] \leftarrow R^F[\sigma] + R^F[\text{pivots}[\ell]]$ 
19:      else
20:        // We saw that column and reduced it
21:        break
22:      if  $R^F[\sigma] \neq 0$  then
23:        pivots[low( $R^F[\sigma]$ )]  $\leftarrow \sigma$ 
24:        if low( $R^F[\sigma]$ )  $\notin [s_{i-1}, s_i]$  then
25:          //  $R^F[\sigma]$  no longer belongs
26:          // to current rank  $i$ , mark it to send further
27:          insert low( $R^F[\sigma]$ ) into updated
28:        else
29:          erase column  $R^F[\sigma]$ 
30:        if  $\sigma_{next} \neq \sigma$  then
31:           $\sigma \leftarrow \sigma_{next}$ 
32:        else
33:          break
34:      return updated
35: end function

```

Algorithm 10 Global Clearing.

```

1: function CLEARCOLUMNS(dim)
2:   for all non-zero columns  $R^F[\tau]$  of  $R^F$  in dimension dim
   do
3:      $\sigma \leftarrow \text{low}(R^F[\tau])$  // Dimension of  $\sigma$  is dim + 1
4:      $r \leftarrow \text{RANKBYVALUE}(\sigma)$ 
5:     send  $\sigma$  to  $r$ 
6:     for all incoming  $\sigma$  do
7:       erase column  $R^F[\sigma]$ 
8: end function

```

the same low). Therefore, if the column of σ happens to be at the same rank, it can be zeroed out immediately. We only need to make sure that we perform reduction in the increasing dimension order. This can be achieved by (stable) sorting the simplices in the filtration with respect to the dimension.

As for the global phase, we choose to explicitly split the matrix into dimension components and perform clearing after we finish each dimension. The reason is that before we enter the global reduction loop (before *SendColumns* is executed), the columns of the matrix in the next dimension are assigned to ranks by their column value. This allows us to easily identify the rank holding the column that we are going to zero out and send the message to this rank only, as in Algorithm 10.

Our experiments show that, while the fraction of the columns zeroed by the global clearing is small, this optimization is crucial in reducing the running time, because those columns would require many more communication rounds to explicitly reduce to zero.

5 EXPERIMENTS

We compare our implementation, called *CADMUS*, with *DIPHA* [2], the only publicly available distributed implementation of persistence. Both codes use MPI; our code uses block-parallel library *DIY* [20] for domain partitioning and exchange between blocks. Experiments were performed on the *Perlmutter* supercomputer (CPU Nodes) at the National Energy Research Scientific Center (NERSC). Every node has 2 AMD Epyc 7763 processors (64 CPU cores, 2.45GHz) and 512 GB of RAM. Our code and *DIPHA* were compiled with Clang 13 specifically optimized by the vendor for AMD processors (AOCC programming environment).

For all the experiments, both *DIPHA* and *CADMUS* use *cubical* complexes, not simplicial ones described in the background. The reduction algorithm remains the same, but the basic blocks are cubes. This approach is much more natural for functions on grids and leads to filtrations of smaller size.

Timings for *DIPHA* are reported according to their own benchmark option. We only take the time for the reduction algorithm itself. Since we use cohomology, we also run *DIPHA* for cohomology.

All dataset files were downloaded from P. Klacansky’s “Open scientific visualization datasets” repository [14]. We used the following data sets.

1. Woodbranch is a microCT scan of a branch of hazelnut.
2. Magnetic reconnection dataset is from [13]. It is a simulation of an interaction between magnetic fields that were concentrated in two different regions and were pointing in two different directions; at the boundary between the regions, magnetic lines change connectivity.
3. Isotropic pressure [26]. The scalar function here is enstrophy. Its high values correspond to regions where the magnitude of the vorticity vector is large.
4. Truss [15] is a simulated CT scan of a truss with some mechanical defects.

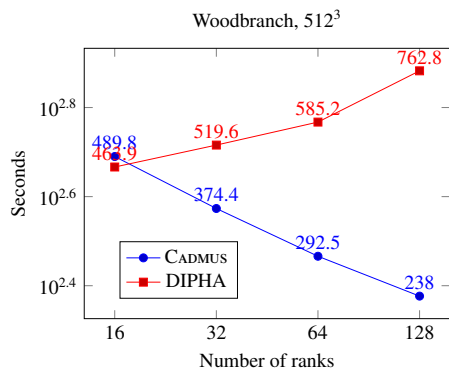


Figure 5: Strong scaling on a 3D scan data (Woodbranch) of size 512^3 . Reduction time only.

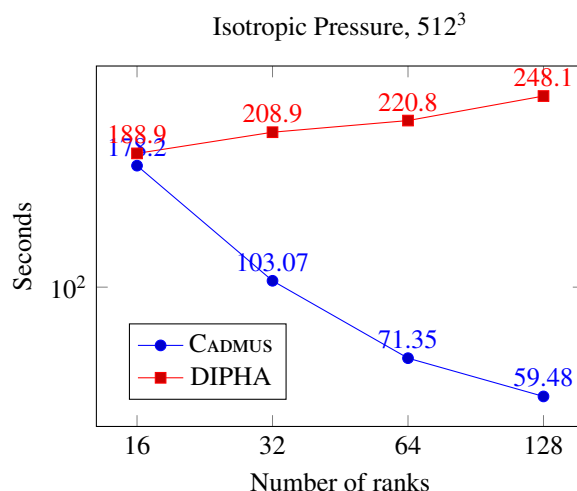


Figure 7: Strong scaling on isotropic pressure data set of size 512^3 . Reduction time only.

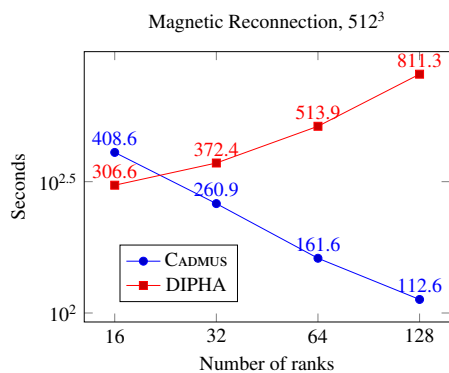


Figure 6: Strong scaling on magnetic reconnection data set of size 512^3 . Reduction time only.

5. Temperature field of the rotating stratified turbulence simulation [25].

The strong scaling plots in Figures 5 to 7 are for 512^3 data sets. In all these examples CADMUS scales significantly better than DIPHA and usually outperforms it. Same holds for Figures 8 and 9, where the size is 1024^3 .

However, the performance is highly dependent on the input, as Figure 10 shows. The Synthetic Truss dataset has very regular and rich topology, as visualized in Figure 11. This figure shows just one particular sublevel set (more precisely, its isosurface). All the 1-cycles that are shown in this figure will be filled in (die) at approximately the same threshold value. Moreover, they are all born at approximately the same threshold value. Hence, whether we distribute the columns according to the low value (birth) or to the column value (death), we will have a great imbalance in the final number of columns among processors. Almost all the work will be done by one rank. The diagram illustrating the distribution of columns at the end of the reduction is in Figure 12. In contrast, Figure 13 shows that for an example that scales well, the columns are distributed uniformly on all processors at the end of the reduction. Persistence diagrams of both data sets are shown in Figures 14 and 15. Note that the Synthetic Truss diagram has 20 times more points and they are highly concentrated in one small domain inside the lower left region, with density higher than 10^6 .

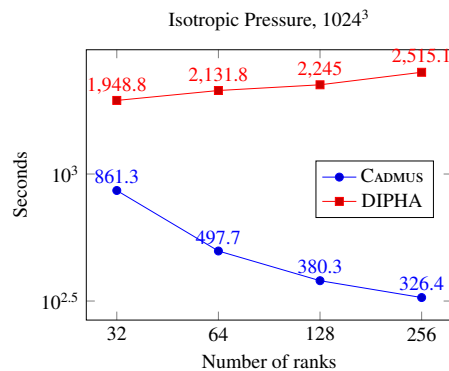


Figure 8: Strong scaling on isotropic pressure data set of size 1024^3 . Reduction time only.

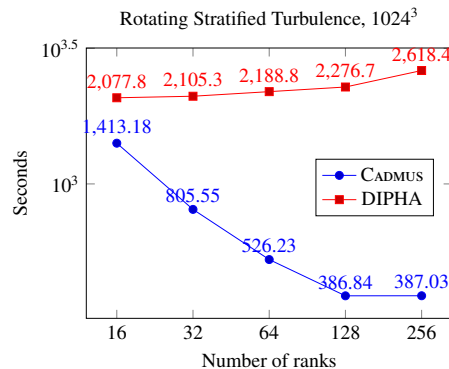


Figure 9: Strong scaling on the temperature field of rotating stratified turbulence simulation data set of size 1024^3 . Reduction time only.

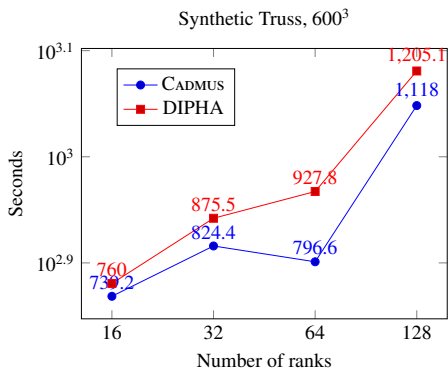


Figure 10: Strong scaling on Synthetic Truss data set of size 600^3 . Reduction time only.

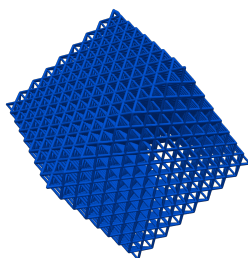


Figure 11: Visualization of Synthetic Truss dataset.

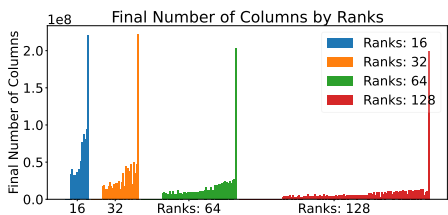


Figure 12: Histogram of the final number of columns on each rank for different number of ranks for Synthetic Truss dataset. One rank dominates all the others.

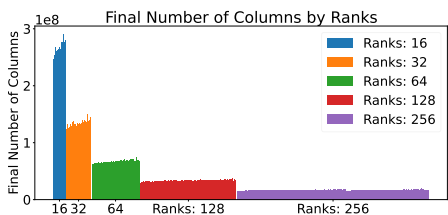


Figure 13: Histogram of the final number of columns on each rank for different number of ranks for rotating stratified turbulence dataset of size 1024^3 . The columns are equally distributed.

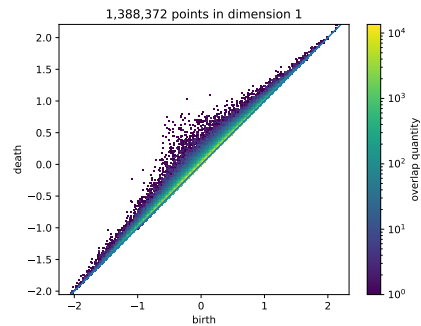


Figure 14: Persistence diagram of the rotating stratified turbulence data set in dimension 1.

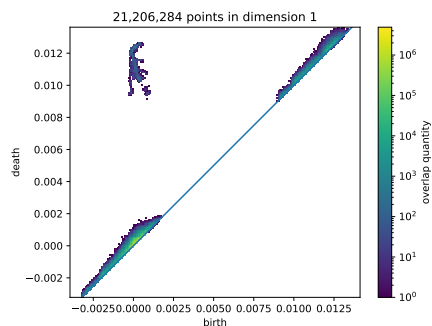


Figure 15: Persistence diagram of the synthetic truss data set in dimension 1.

It is difficult to evaluate weak scaling for persistence computation for lack of suitable data. If one takes a large data set and cuts out a small subset, one inevitably loses large-scale features that often take the most of time to process. If one coarsens the data set by smoothing, the numerous fine-scale features get eliminated. Nonetheless, we investigated the weak scaling properties of our algorithm following the second procedure. Specifically, we downsampled a 1024^3 dataset to sizes 512^3 and 256^3 by averaging over $2 \times 2 \times 2$ voxels. Dividing the number of processors by 8 each time, each rank gets the same amount of input data. However, since persistence diagram also captures global characteristics of the input, and we effectively smoothed it, removing lots of topological features, one cannot expect ideal weak scaling. That is indeed the case for the temperature field of turbulence simulation, plotted in Figure 16. The running time is multiplied first by a factor of 2; second, by almost a factor of 4 for CADMUS.

6 CONCLUSION

We presented a new distributed algorithm for computing persistent cohomology. It combines space and range partitioning and avoids computing the Mayer–Vietoris blowup complex. Reducing data locally before switching to the global reduction is beneficial for scaling, but as always with topological computation, the performance is data-dependent. For grossly unbalanced inputs, the computation scales poorly with increasing number of processors.

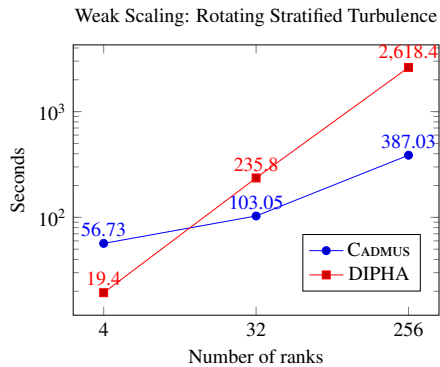


Figure 16: Weak scaling on the temperature field of rotating stratified turbulence simulation: data sets of size 256^3 , 512^3 and 1024^3 .

Overcoming the data-dependent imbalance of our algorithm is one of the most pressing issues for future work. We may also be able to improve the efficiency of our implementation by experimenting with different data structures for column addition. This choice can have a significant impact on the running time [3].

Although we don't discuss it in this work, persistent cohomology is known to be particularly efficient for computing persistence of Vietoris–Rips filtrations [8, 1], which makes our algorithm particularly promising for tackling large problems in that domain. Before doing so, we have to solve other subproblems involved in that computation, specifically, the efficient construction of (spatially localized) cliques in the near-neighbor graphs. We leave this as a direction for future research.

There are applications of persistence that rely on access to cocycles [9]. They immediately benefit from our new algorithm. At the same time, there are applications that need access to both cycles and cocycles (as well as their bounding chains and cochains) [22]. In other words, they need both homology and cohomology computation. Adapting our algorithm to the homology setting is another important future research direction. We use the cohomology implementation in DIPHA to get a fair comparison, but experiments with its homology implementation suggest that it is better suited for the data sets used in this paper.

ACKNOWLEDGMENT

This work was supported by the U.S. Department of Energy, Office of Science, Office of Advanced Scientific Computing Research, Scientific Discovery through Advanced Computing (SciDAC) program and Mathematical Multifaceted Integrated Capability Centers (MMICCs) program, under Contract No. DE-AC02-05CH11231 at Lawrence Berkeley National Laboratory. This research used resources of the National Energy Research Scientific Computing Center (NERSC), a U.S. Department of Energy Office of Science User Facility using NERSC award ASCR-ERCAP-28617. This research used the Lawrence computational cluster resource provided by the IT Division at the Lawrence Berkeley National Laboratory (Supported by the Director, Office of Science, Office of Basic Energy Sci-

ences, of the U.S. Department of Energy under Contract No. DE-AC02-05CH11231).

REFERENCES

- [1] Ulrich Bauer. Ripser: efficient computation of Vietoris–Rips persistence barcodes. *Journal of Applied and Computational Topology*, June 2021.
- [2] Ulrich Bauer, Michael Kerber, and Jan Reininghaus. Distributed computation of persistent homology. In *2014 proceedings of the sixteenth workshop on algorithm engineering and experiments (ALENEX)*, pages 31–38. SIAM, 2014.
- [3] Ulrich Bauer, Michael Kerber, Jan Reininghaus, and Hubert Wagner. Phat–persistent homology algorithms toolbox. *Journal of symbolic computation*, 78:76–90, 2017.
- [4] Álvaro Torras Casas. Distributing persistent homology via spectral sequences. *arXiv [math.AT]*, July 2019.
- [5] Chao Chen and Michael Kerber. Persistent homology computation with a twist. In *Proceedings 27th European workshop on computational geometry*, volume 11, pages 197–200, 2011.
- [6] Chao Chen, Xiuyan Ni, Qinxun Bai, and Yusu Wang. A topological regularizer for classifiers via persistent homology. In *The 22nd International Conference on Artificial Intelligence and Statistics*, pages 2573–2582. PMLR, 2019.
- [7] David Cohen-Steiner, Herbert Edelsbrunner, and Dmitriy Morozov. Vines and vineyards by updating persistence in linear time. In *Proceedings of the twenty-second annual symposium on Computational geometry*, pages 119–126, 2006.
- [8] Vin de Silva, Dmitriy Morozov, and Mikael Vejdemo-Johansson. Dualities in persistent (co)homology. *Inverse problems*, 27(12):124003, November 2011.
- [9] Vin de Silva, Dmitriy Morozov, and Mikael Vejdemo-Johansson. Persistent cohomology and circular coordinates. *Discrete & computational geometry*, 45(4):737–759, June 2011.
- [10] Edelsbrunner, Letscher, and Zomorodian. Topological persistence and simplification. *Discrete & computational geometry*, 28:511–533, 2002.
- [11] H Edelsbrunner and J Harer. Persistent homology — a survey. *Contemporary Mathematics*, 2008.
- [12] Herbert Edelsbrunner and Dmitriy Morozov. Persistent homology. In Jacob E Goodman, Joseph O’Rourke, and Csaba D Tóth, editors, *Handbook of Discrete and Computational Geometry*. CRC Press, 2017.
- [13] Fan Guo, Hui Li, William Daughton, and Yi-Hsin Liu. Formation of hard power laws in the energetic particle spectra resulting from relativistic magnetic reconnection. *Phys. Rev. Lett.*, 113:155005, October 2014.
- [14] Pavol Klacansky. Open scientific visualization datasets. <https://klacansky.com/open-scivis-datasets>, 2021.

- [15] Pavol Klacansky, Haichao Miao, Attila Gyulassy, Andrew Townsend, Kyle Champley, Joseph Tringe, Valerio Pascucci, and Peer-Timo Bremer. Virtual inspection of additively manufactured parts. In *2022 IEEE 15th Pacific Visualization Symposium (PacificVis)*, pages 81–90, 2022.
- [16] Aditi S Krishnapriyan, Maciej Haranczyk, and Dmitriy Morozov. Topological descriptors help predict guest adsorption in nanoporous materials. *Journal of Physical Chemistry C*, 124(17):9360–9368, April 2020.
- [17] Ryan Lewis and Dmitriy Morozov. Parallel computation of persistent homology using the blowup complex. In *Proceedings of the 27th ACM Symposium on Parallelism in Algorithms and Architectures*, pages 323–331, 2015.
- [18] Rodrigo Mendoza-Smith and Jared Tanner. Parallel multi-scale reduction of persistent homology filtrations. *arXiv [math.AT]*, August 2017.
- [19] Dmitriy Morozov and Arnur Nigmatov. Towards lockfree persistent homology. In *Proceedings of the 32nd ACM Symposium on Parallelism in Algorithms and Architectures*, pages 555–557, 2020.
- [20] Dmitriy Morozov and Tom Peterka. Block-parallel data analysis with DIY2. In *2016 IEEE 6th Symposium on Large Data Analysis and Visualization (LDAV)*, pages 29–36. IEEE, 2016.
- [21] Arnur Nigmatov, Aditi Krishnapriyan, Nicole Sanderson, and Dmitriy Morozov. Topological regularization via persistence-sensitive optimization. *Computational Geometry*, page 102086, 2024.
- [22] Arnur Nigmatov and Dmitriy Morozov. Topological optimization with big steps. *Discrete & Computational Geometry*, pages 1–35, January 2024.
- [23] Pratyush Pranav, Herbert Edelsbrunner, Rien van de Weygaert, Gert Vegter, Michael Kerber, Bernard J T Jones, and Mathijs Wintraecken. The topology of the cosmic web in terms of persistent betti numbers. *Monthly notices of the Royal Astronomical Society*, 465(4):4281–4310, March 2017.
- [24] Jan Reininghaus, Ulrich Bauer, and Michael Kerber. DIPHA: A Distributed Persistent Homology Algorithm. <https://github.com/DIPHA/dipha>, 2014–2016.
- [25] Duane Rosenberg, Annick Pouquet, Raffaele Marino, and Pablo Daniel Mininni. Evidence for bolgianobukhov scaling in rotating stratified turbulence using high-resolution direct numerical simulations. *Physics of Fluids*, 27(5), 2015.
- [26] PK Yeung, DA Donzis, and KR Sreenivasan. Dissipation, enstrophy and pressure statistics in turbulence simulations at high Reynolds numbers. *Journal of Fluid Mechanics*, 700:5, 2012.
- [27] Simon Zhang, Mengbai Xiao, Chengxin Guo, Liang Geng, Hao Wang, and Xiaodong Zhang. HYPHA: A framework based on separation of parallelisms to accelerate persistent homology matrix reduction. In *Proceedings of the ACM International Conference on Supercomputing*, pages 69–81, 2019.